Available online at www.sciencedirect.com
ScienceDirect
Trans. Nonferrous Met. Soc. China 28(2018) 687−699
Transactions of Nonferrous Metals Society of China
www.tnmsc.cn

Synthesis of biodegradable Mg−Zn alloy by mechanical alloying: Statistical prediction of elastic modulus and mass loss using fractional factorial design

Emee Marina SALLEH[1,2], Hussain ZUHAILAWATI[1], Sivakumar RAMAKRISHNAN[1]

1. Biomaterials Niche Area, School of Materials and Mineral Resources Engineering, Engineering Campus, Universiti Sains Malaysia, 14300 Nibong Tebal, Penang, Malaysia;
2. School of Applied Physics, Faculty of Science and Technology, Universiti Kebangsaan Malaysia, 43600 UKM Bangi, Selangor, Malaysia

Received 7 December 2016; accepted 17 April 2017

Abstract: Biodegradable Mg−Zn alloy was synthesized using mechanical alloying where a statistical model was developed using fractional factorial design to predict elastic modulus and mass loss of the bulk alloy. The effects of mechanical alloying parameters (i.e., milling time, milling speed, ball-to-powder mass ratio and Zn content) and their interactions were investigated involving 4 numerical factors with 2 replicates, thus 16 runs of two-level fractional factorial design. Results of analysis of variance (ANOVA), regression analysis and R^2 test indicated good accuracy of the model. The statistical model determined that the elastic modulus of biodegradable Mg−Zn alloy was between 40.18 and 47.88 GPa, which was improved and resembled that of natural bone (30−57 GPa). Corrosion resistance (mass loss of pure Mg, 33.74 mg) was enhanced with addition of 3%−10% Zn (between 9.32 and 15.38 mg). The most significant independent variable was Zn content, and only the interaction of milling time and ball-to-powder mass ratio was significant as P-value was less than 0.05. Interestingly, mechanical properties (represented by elastic modulus) and corrosion resistance (represented by mass loss) of biodegradable Mg−Zn alloy can be statistically predicted according to the developed models.

Key words: biodegradable Mg−Zn alloy; mechanical alloying; fractional factorial design; elastic modulus; mass loss

1 Introduction

Recently, magnesium (Mg) and its alloys have attracted increasing attention as innovative biodegradable materials, particularly for their potential use as temporary orthopedic implants and coronary stents. Mg alloys have shown potential for use in biodegradable materials due to their excellent biological performance and biodegradability in the bioenvironment [1]. In terms of mechanical properties, Mg is very compatible with natural bone. Its density (1.74 g/cm^3) and elastic modulus (45−48 GPa) are closer to those of bone (1.8−2.1 g/cm^3 and 30−57 GPa) [2] than in the case of other currently used biomaterials for fixation of fractured bone, like titanium (Ti) alloys, stainless steels or cobalt−chromium (Co−Cr) alloys (approximately 100, 180 and 210 GPa, respectively) [3,4]. For biocompatibility, a large number of Mg ions are present in the human body and are involved in many metabolic reactions and biological mechanisms. The human body usually contains approximately 35 g Mg per 70 kg body, and the daily dietary demand for Mg is about 375 mg [5]. Mg-based biomaterials have been demonstrated to stimulate the formation of new tissue when they are implanted as bone fixtures. It has been accepted that there are no serious concerns regarding the harm that can be caused by Mg ions to the human body [6]. However, Mg-based biomaterials are susceptible to attack in chloride-containing solutions, such as the human body fluid or blood plasma [7].

The most effective way to improve mechanical integrity and degradation behavior of Mg is by alloying with additional elements. Mechanically, zinc (Zn) strengthens Mg alloys and, importantly, Zn could enhance both corrosion potential and Faraday charge transfer resistance of Mg, thus improving corrosion resistance [3]. Clinically, Zn is an essential trace element in the human body, and compared with several other metal ions with similar chemical properties, Zn is relatively harmless [8]. Hence, in this study Zn was chosen as the alloying element and incorporated into the

Corresponding author: Hussain ZUHAILAWATI; Tel: +60-45995258; Fax: +60-45941011; E-mail: zuhaila@usm.my
DOI: 10.1016/S1003-6326(18)64701-6

Mg matrix with the aim of improving mechanical properties and reducing corrosion rate of Mg.

Recently, the use of powder metallurgy (PM) coupled with mechanical alloying (MA) to synthesize Mg-based alloys is a field of growing interest. This technique is a solid state powder metallurgical process in which elemental powders are alloyed by a repeated deformation mechanism under frequent mechanical impacts [9,10]. MA is one of the simplest and most economical routes for the fabrication of nanocrystalline biometallic materials. In this current work, binary Mg−Zn alloy was produced using mechanical alloying (MA) followed consolidation process by compaction and sintering.

Regularly conventional research methodology via trial and error method is adopted to ascertain the important processing conditions, but certainly, this methodology is both costly and time-consuming for the volume or number of experimental work to be performed [11,12]. Thus, to screen out MA parameters in preparing Mg−Zn alloy we used the design of experiment (DOE) method. This approach helps to understand better how the change in the levels of application of a group of parameters affects the response [13]. When certain high-order interactions are probably negligible, information on the main effects and low-order interactions may be obtained by running only a fraction of complete factorial design [14,15]. Of the available method, a fractional factorial design (FFD) is the most widely used types of design for product and process design and for process improvement. Interestingly, the FFD is a variation of the basic factorial design in which only a subset of the run is used. In developing the regression equation, the test variables were coded according to the following equation:

$$X_j=(Z_j-Z_{0j})/\Delta_j \quad (1)$$

where X_j is the coded value of independent variable, Z_j is the real value of the independent variable, Z_{0j} is the value of independent variable on center point and Δ_j is the step change value. The linear model can be expressed as follows:

$$Y=\beta_o\sum_{j=1}^{n}\beta_j X_j \quad (2)$$

where Y is the predicted response, β_o is the intercept, β_j is the jth linear coefficient and X_j is the input variable which influences the response.

Referring to the present work, the FFD method enables the establishment of the polynomial functions that describe the effects of MA processing conditions on the final properties of Mg−Zn alloy, knowledge of which is beneficial in further use of fabrication of Mg−Zn alloy. Interestingly, only a fraction of actual experiment number is required to be run without forfeiting the accuracy of the final properties [12]. To sum up, high accuracy of developed mathematical models can quantify the experimental output efficiently and economically using FFD.

2 Experimental

2.1 Materials preparation and characterization

A mixture of elemental Mg (99.00% purity) and Zn (99.70% purity) powders was mechanically milled at room temperature using a high-energy Fritsch Pulveristte P-5 planetary mill under argon atmosphere. The particle size of the powder was measured by particle size analyzer using Helos (H1938) & Rodos equipment. The measurement was carried out in dry condition as the Mg−Zn powder is very reactive to humidity. SEM micrographs of the starting Mg and Zn powders are shown in Fig. 1. Mg powders are irregular-shaped and Zn powders are mostly ellipsoidal, elongated particles.

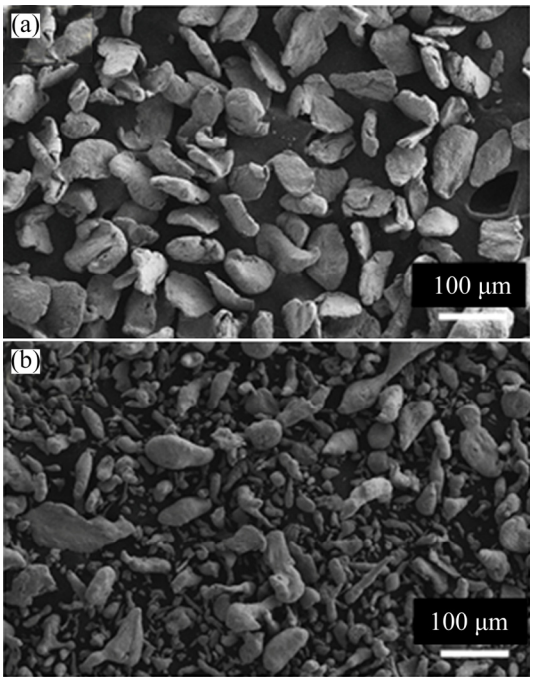

Fig. 1 SEM images of elemental Mg (a) and Zn (b) powders

The particle sizes of elemental Mg powder and Zn powders are up to 227.41 μm and 121.65 μm respectively, as listed in Table 1. 20 mm-diameter stainless steel balls were used during mechanical alloying. 3% *n*-heptane was added to the powder mixture prior to the milling process to prevent excessive cold welding of the elemental alloy powders.

Then, the milled powders were uniaxially cold pressed under 400 MPa for 2 min at room temperature to produce 10 mm-diameter of green Mg−Zn alloy compacts and sintered at 350 ºC under argon flow at

Table 1 Distribution of average particle size of Mg and Zn powders

Powder	D_{10}/μm	D_{50}/μm	D_{90}/μm
Mg	61.33	102.63	227.41
Zn	27.60	65.81	121.65

10 °C/min with both heating and cooling rates for 1 h in order to form green solid bodies. Qualitative X-ray diffraction (XRD) analysis with angular scanning range $20°\leq 2\theta \leq 90°$ was conducted to identify the presence of elements and phases. The data attained were analyzed using D8 Advance, Bruker AXS. Phase identification of stripping its $K_{\alpha 2}$ component is represented in the form of a diffractogram of intensity versus 2θ. APW software was used to analyze the present phase in all samples. Internal strain was determined by the Williamson–Hall method as shown in the following equation:

$$B_r \cos\theta = \frac{0.89\lambda}{\langle D \rangle} + 2\eta \sin\theta \quad (3)$$

where B_r is the line broadening, θ is the Bragg's angle, λ is the wavelength, D is the crystallite size and η is the internal strain. The instrumental broadening B_i was removed using the Gaussian profile:

$$B_r^2 = B^2 - B_i^2 \quad (4)$$

where B is the full width at half maximum.

Mechanical testing was performed according to ASTM E9−09 for standard test methods of compression testing of metallic materials at room temperature using a universal testing machine (Instron 5982). A cylindrical sample of sintered compacts with 10 mm in height and 10 mm in length was prepared. Compression characteristics were tested at constant cross head speed and a strain rate of 0.5 mm/min at room temperature. All mechanical tests were repeated five times using universal tensile machine.

Prior to mass loss measurement, the samples were ground with SiC emery paper up to 2000 grit and then polished with 1 μm diamond paste. The polished samples were ultrasonically cleaned in 90% ethanol and dried under warm airflow. The samples of 10 mm in diameter and 2 mm in thickness were weighed using four-decimal electronic analytical balance (Sartorius) before immersion (m_0) in a 3.5% NaCl solution. After 3 d of immersion, the samples were removed from the solution. The samples were cleaned with a dilute chromic acid (a mixture of CrO_3 and $AgNO_3$) to remove the corrosion layer by dissolving $Mg(OH)_2$ compound and rinsed with ethanol followed by de-ionized water. Then, the samples were put in a dryer at 60 °C for 24 h. Finally, the mass of the dried samples (m_f) was measured and the mass loss (m_l) was calculated according to

$$m_l = m_0 - m_f \quad (5)$$

2.2 Statistical design

A combination of levels of the parameters that leads to a certain optimum response can be identified through the factorial design approach [11]. Previous studies [8,12,15] have reported that there were a large number of mechanical alloying factors that have a significant influence on the properties of mechanically alloyed soft metal powder. However, to reduce the complexity of the high energy milling parameters, this study focused only on the effects of milling time, milling speed (energy), and ball-to-powder ratio (BPR) as well as Zn content on the properties of Mg. Factors and levels evaluated in the DOE are listed in Table 2. The upper limits of milling time, milling speed, BPR and content of Zn were set as 10 h, 300 r/min, 15:1 and 10%, respectively, according a preliminary study whose results have not been published. The upper limits were set with the intention of avoiding excessive cold welding of powder during milling that could hinder powder densification.

Table 2 Factors and levels evaluated in experiment

Factor	Code	Unit	Level	
			Low	High
Milling time	*A*	h	2	10
Milling speed	*B*	r/min	100	300
BPR	*C*		5:1	15:1
Zn content	*D*	%	3	10

In this study, the experimental procedure followed a 2^{k-1} FFD, that is, a series of experiments involving k factors, each of which has two levels (low level as −1 and high level as +1). It is one of the main interests to highlight the usefulness of this FFD method. Since the work involves 4 factors, a design using fractional factorial of 2 levels was applied to minimizing the number of experimental runs without sacrificing its accuracy so that the properties prediction of binary Mg−Zn alloy could be economically attained in a short period of time. Table 2 shows the complete experimental design and actual responses of the experiment used in this study. The actual responses for elastic modulus and mass loss are denoted by Y_1 and Y_2, respectively. Since the design was constructed involving 4 numerical factors with 2 replicates, 16 runs of 2-level FFD were performed.

These experimental data were used as input into the DOE for analysis to determine the model equation. The Minitab 16 (Minitab Inc, USA) statistical software was used to perform statistical analysis and to develop the empirical model. The adequacy of the model was further justified through analysis of variance (ANOVA), regression analysis and R^2 test. According to the design, the generator of defining relation (D) for FFD is equal to ABC.

3 Results and discussion

3.1 Phase and microstructure analysis

Figure 2 illustrates the XRD patterns for a set of replications chosen. The XRD patterns of all mechanically alloyed sintered compacts produced according to the created design showed the presence of α-Mg phase. Since samples 1, 4, 6 and 7 were alloyed with only 3% Zn, approximately all the added alloying element (Zn) was solid-solved into the host Mg, forming α-Mg solid solution. In this alloy system, the solubility limit of Zn in Mg phase is 6.2% at 340 °C, but the solubility is very low at room temperature. Since only single α-Mg phase was observed in the Mg−Zn alloy matrix, the result clearly suggested that Mg and Zn formed a homogeneous solid solution due to the diffusive reaction that occurred between pure metals without the formation of intermetallic compound or intermediate phase alloy (secondary solid solution) [16]. However, the presence of α-Mg and γ-MgZn phase peaks can be clearly identified in samples 2, 3, 5 and 8. These four sintered compacts were alloyed with 10% Zn. The amount of Zn added into the Mg matrix was high, exceeding its solubility limit, thus accounting for the high likelihood for the formation of secondary phase γ-MgZn.

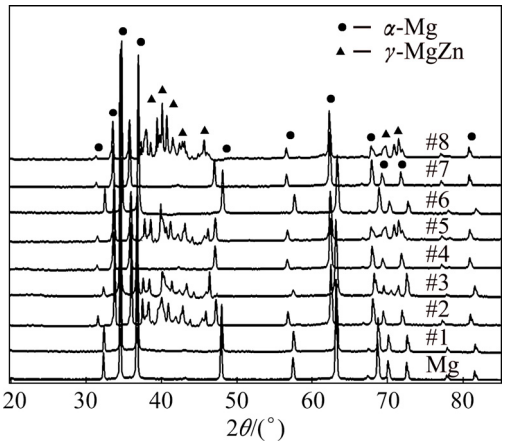

Fig. 2 XRD patterns of sintered Mg−Zn alloy

Typical micrographs of Mg-based alloys with different Zn contents are presented in Fig. 3. Note that a single phase of α-Mg was observed in Mg−3%Zn alloy whereas a white precipitate corresponding to γ-MgZn phase was observed in the α-Mg matrix of Mg−10%Zn alloy. Figure 2 shows that most of the peaks of the sintered alloys shifted to the left (lower Bragg's angle) with the formation of α-Mg solid solution. During the formation of the solid solution, Zn atoms of smaller radius (134 pm) appeared as impurities in the larger (157 pm) Mg atom lattice. The replacement of Zn in the

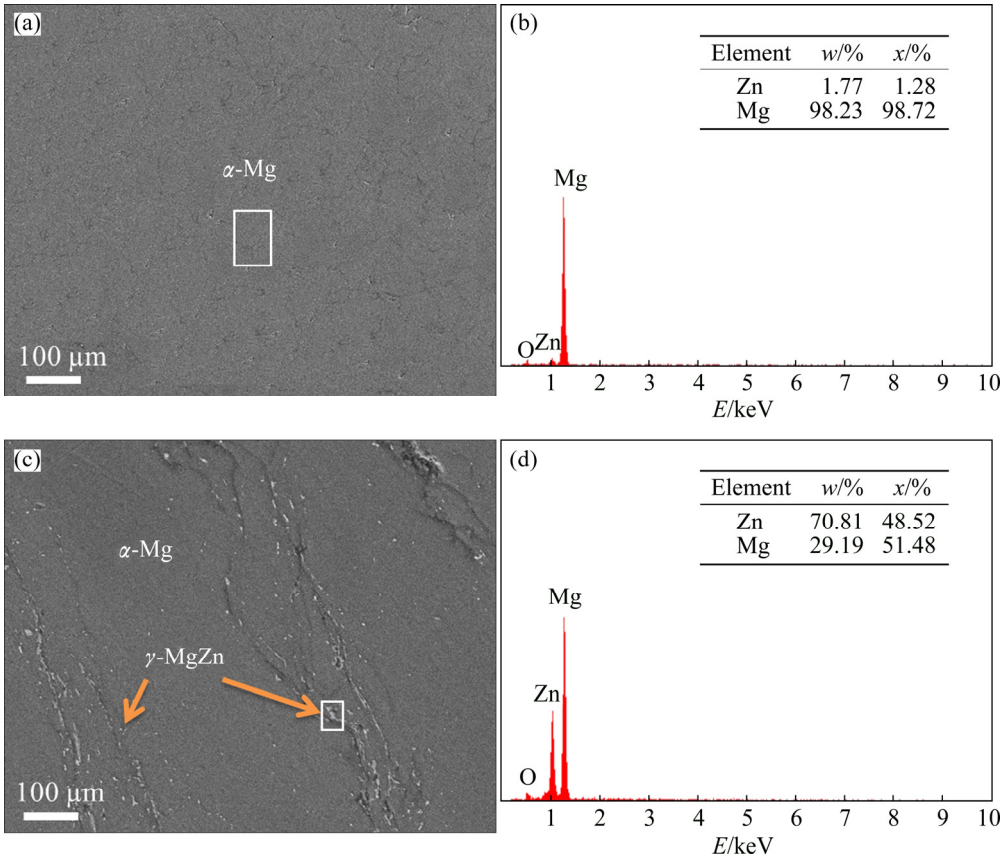

Fig. 3 Micrographs (a, c) and EDX profiles (b, d) of Mg−3%Zn (a, b) and Mg−10%Zn (c, d) alloys

host sites caused a reduction of the Mg lattice. In addition, the shifted angles were also caused by a reduction of crystallite size and/or the accumulation of lattice strain during mechanical alloying, indicating that the formation of fine crystallite was typically affected by increasing the number of collisions per unit time during the milling process [17,18].

3.2 Analysis of variance of fractional factorial design

The aim of this study was to fabricate new biodegradable Mg-based alloy as a biocompatible implant with maximized elastic modulus of Mg−Zn alloy and minimized mass loss in the most corrosive environment to Mg (solution containing Cl^- ions), which corresponds to enhancement of its corrosion resistance. Table 3 shows a complete experimental design and actual responses of the experiment used in this study. Only a slight change of elastic modulus for all sixteen Mg−Zn sintered compacts was attained. The values lay between 40 and 48 GPa, which is considerably acceptable since the reported elastic modulus of human bone is between 30 and 57 GPa [2,19]. Most importantly, the mass loss of pure Mg was efficiently reduced with the addition of Zn, even at a level as low as 3%, produced using a designed combination of factors. The mass loss of pure mechanically milled Mg is 33.74 mg after immersion in the 3.5% NaCl solution. However, according to the created design, the mass loss of Mg−Zn alloy was commendably reduced to 9.32 mg. This reduction in mass loss indicated that addition of Zn with a proper combination of mechanical alloying parameters significantly enhanced corrosion resistance of pure Mg, thus lowering its degradation rate, which is especially desirable during the implantation period.

After completion of data collection, the results were analyzed for adequacy using analysis of variance (ANOVA) for both elastic modulus (Y_1, Table 4) and mass loss (Y_2, Table 5). Statistical effects of variables were calculated within 95% confidence interval. The *F*-value of 195.13 for elastic modulus and 55.47 for mass loss implied that the models which were represented in Eqs. (6) and (7) were significant relative to noise. For both properties, there was only 0.001% chance that the *F*-value model may fail due to noise for each case.

To obtain the best-fit model to the experimental data, a regression analysis for each response was performed using coded units, and the findings are summarized in Tables 6 and 7. According to the regression analysis, all of the studied factors were significant on both responses of elastic modulus and mass loss as *P*-value was less

Table 3 2^{4-1} experimental design and actual responses of binary Mg−Zn alloy

Run	Basic design				(Y_1) Elastic modulus/GPa	(Y_2) Mass loss/mg
	A	*B*	*C*	*D*=*ABC*		
1	−	−	−	−	41.83	13.74
2	+	−	−	+	45.24	10.76
3	−	+	−	+	47.88	9.32
4	+	+	−	−	44.16	11.85
5	−	−	+	+	46.47	10.54
6	+	−	+	−	40.18	15.74
7	−	+	+	−	43.79	12.89
8	+	+	+	+	45.38	12.28
9	−	−	−	−	42.61	13.63
10	+	−	−	+	45.63	11.87
11	−	+	−	+	47.86	10.18
12	+	+	−	−	44.27	12.57
13	−	−	+	+	45.62	10.96
14	+	−	+	−	40.25	15.38
15	−	+	+	−	43.87	12.63
16	+	+	+	+	45.56	12.14

Table 4 Analysis of variance of elastic modulus (coded units)

Source	DF	Seq SS	Adj SS	Adj MS	*F*	*P*
Main effect	4	75.0865	75.0865	18.7716	195.13	0.000
Milling time	1	5.3592	5.3592	5.3592	55.71	0.000
Milling speed	1	13.9502	13.9502	13.9502	145.01	0.000
BPR	1	4.3681	4.3681	4.3681	45.41	0.000
Zinc content	1	51.4089	51.4089	51.4089	534.40	0.000
2-way interactions	3	4.0886	4.0886	1.3629	14.17	0.001
Milling time and milling speed	1	0.0900	0.0900	0.0900	0.94	0.362
Milling time and BPR	1	3.5156	3.5156	3.5156	36.54	0.000
Milling time and zinc content	1	0.4830	0.4830	0.4830	5.02	0.055
Residual error	8	0.7696	0.7696	0.0962		
Pure error	8	0.7696	0.7696	0.0962		
Total	15	79.9447				

DF—Degree of freedom; Seq SS—Sequential sum of square; Adj SS—Adjusted sum of square; Adj MS—Adjusted mean square

than its confidence level (i.e., α=95%, $P\leq$0.05). Zn content provided the lowest P-value, indicating that it was the most significant factor. Then, it is followed by milling speed, milling time and BPR.

In addition, coefficient of correlation (R^2) test is one of the most conveniently reliable methods which allow to examine the fitted model to ensure that it provides an adequate approximation to the true system and verify that none of the least squares regression assumptions are violated [20]. R^2 value gives a correlation between the experimental and predicted responses and should be high for a particular model to be significant. R^2 values for

Table 5 Analysis of variance of mass loss (coded units)

Source	DF	Seq SS	Adj SS	Adj MS	F	P
Main effect	4	40.1514	40.1514	10.0378	55.47	0.000
Milling time	1	4.7306	4.7306	4.7306	26.14	0.001
Milling speed	1	4.7961	4.7961	4.7961	26.50	0.001
BPR	1	4.6656	4.6656	4.6656	25.78	0.001
Zinc content	1	25.9590	25.9590	25.9590	143.45	0.000
2-way interactions	3	5.1400	5.1400	1.7133	9.47	0.005
Milling time and milling speed	1	0.0702	0.0702	0.0702	0.39	0.551
Milling time and BPR	1	4.3472	4.3472	4.3472	24.02	0.001
Milling time and zinc content	1	0.7225	0.7225	0.7225	3.99	0.081
Residual error	8	1.4477	1.4477	0.1810		
Pure error	8	1.4477	1.4477	0.1810		
Total	15	46.7390				

Table 6 Effect and regression coefficient of elastic modulus (Y_1)

Term	Effect	Coef	SE coef	T	P
Constant		44.4125	0.07754	572.77	0.000
Milling time	−1.1575	−0.5787	0.07754	−7.46	0.000
Milling speed	1.8675	0.9337	0.07754	12.04	0.000
BPR	−1.0450	−0.5225	0.07754	−6.74	0.000
Zinc content	3.5850	1.7925	0.07754	23.12	0.362
Milling time and milling speed	0.1500	0.0750	0.07754	0.97	0.000
Milling time and BPR	−0.9375	−0.4687	0.07754	−6.05	0.055
Milling time and zinc content	−0.3475	−0.1737	0.07754	−2.24	

S=0.310161 PRESS=3.0784

R^2=99.04% R^2(pred)=96.15% R^2(adj)= 98.20%

Lack of fit=1.278

Effect—Factors or interactions effect; Coef—Regression coefficient; SE coef—Standard error of coefficient; T—Ratio of coefficient to standard error

Table 7 Effect and regression coefficient of mass loss (Y_2)

Term	Effect	Coef	SE coef	T	P
Constant		12.280	0.1063	115.47	0.000
Milling time	1.087	0.544	0.1063	5.11	0.001
Milling speed	−1.095	−0.547	0.1063	−5.15	0.001
BPR	1.080	0.540	0.1063	5.08	0.001
Zinc content	−2.548	−1.274	0.1063	−11.98	0.000
Milling time and milling speed	−0.133	−0.066	0.1063	−0.62	0.551
Milling time and BPR	1.043	0.521	0.1063	4.90	0.001
Milling time and zinc content	0.425	0.212	0.1063	2.00	0.081

S=0.425397 PRESS=5.7908

R^2=96.90% R^2(pred)=87.61% R^2(adj)= 94.19%

Lack of fit=0.925

elastic modulus and mass loss were 99.04% and 96.90%, respectively, with very small standard deviations of 0.310161 and 0.425397, respectively. The high R^2 values implied that all responses were fairly closer to the predicted values and thus the regression equation generated in this experimental study could adequately be used in the prediction of properties of binary Mg−Zn alloy with a fair degree of accuracy. Furthermore, the obtained data showed that the predicted R^2 values were in good agreement with the adjusted R^2 values for both responses. The regression analysis suggested that the relationship between both responses of binary Mg−Zn alloy and the four factors was best fitted with a partial quadratic model. For each response, the coded models are listed as follows:

$$Y_1=44.413-0.579A+0.934B-0.523C+1.793D+0.075AB-0.469AC-0.174AD \quad (6)$$

$$Y_2=12.280+0.544A-0.547B+0.540C-1.274D-0.066AB+0.521AC+0.212AD \quad (7)$$

The first order of the developed model showed that the lack of fits of both responses was not significant (>0.05%), indicating that the accuracy of the models with only 0.96% (elastic modulus) and 3.10% (mass loss) of the total variation could not be explained by the model. Therefore, the reduction of the model was unnecessarily required. As a matter of fact, the adequacy of the regression model in Eqs. (6) and (7) was also matched with the half normal plot of the standardized effects (Fig. 4). In Fig. 4, the half normal graphs studied at significance level denoted as alpha equal to 0.05 were plotted for Y_1 and Y_2 as responses. As can be seen, the straight line in both plots represented the linear mathematical model. The interception indicates that the factors are insignificant and the points lie farther from the line or off the line shows that the factors are more significant [21]. In this study, all the studied factors and only one low level interaction were significant on both responses. For this kind of plots, it could be simply understood that the marks laid on the left side of the straight line gave negative effect on the response while the marks laid on the right side of the straight line gave positive effect on the response. According to the attained standardized effect, it was found that the elastic modulus of Mg−Zn alloy could be enhanced by increasing milling speed and Zn content, on the other hand reducing milling time and BPR. The same tendency was also found for lowering mass loss which was by increasing milling speed and Zn content while reducing milling time and BPR.

The importance of factors and interactions could be graphically interpreted by constructing Pareto chart. Pareto chart is a bar graph arranged in descending length from top to bottom. The bars not only represent

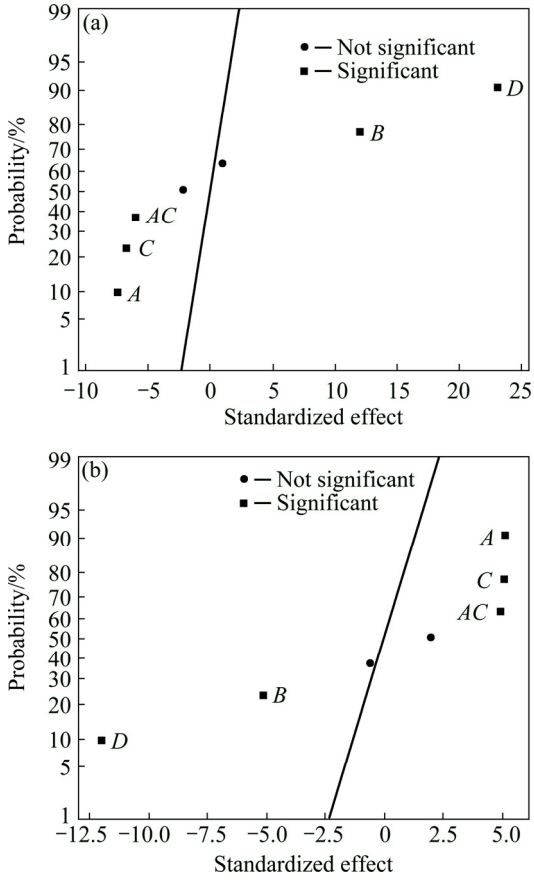

Fig. 4 Half normal plot of standardized effects for elastic modulus (a) and mass loss (b)

frequency but denote significance of the investigated factors and related interactions as well. In this way the chart visually depicts whose situations are more significant. Figure 5 clearly exhibited that factor *D* (Zn content) was the most significant factor on both elastic modulus and mass loss which followed by factors *B* (milling speed), *A* (milling time) and *C* (BPR). This chart also showed that only interaction *AC* was significant. These factors and interaction were considerably significant as the standardized effects were greater than the margin error of 2.31. Although the interactions of *AB* and *AD* were clearly insignificant, these interactions could not be rejected from the model since the interacted factors were independently influential on both responses. Concisely, in order to maximize the elastic modulus and minimize mass loss of the biodegradable Mg−Zn alloy, *B* and *D* have to be increased while *A* and *C* need to be reduced.

The effects of principal factors and interaction between parameters on the elastic modulus and mass loss of biodegradable Mg−Zn alloy were studied. According to the sparsity of effect principle in factorial design, it was most likely that main (single factor) effects and 2-factor interactions were the most significant effects, and the higher order interactions were negligible. In

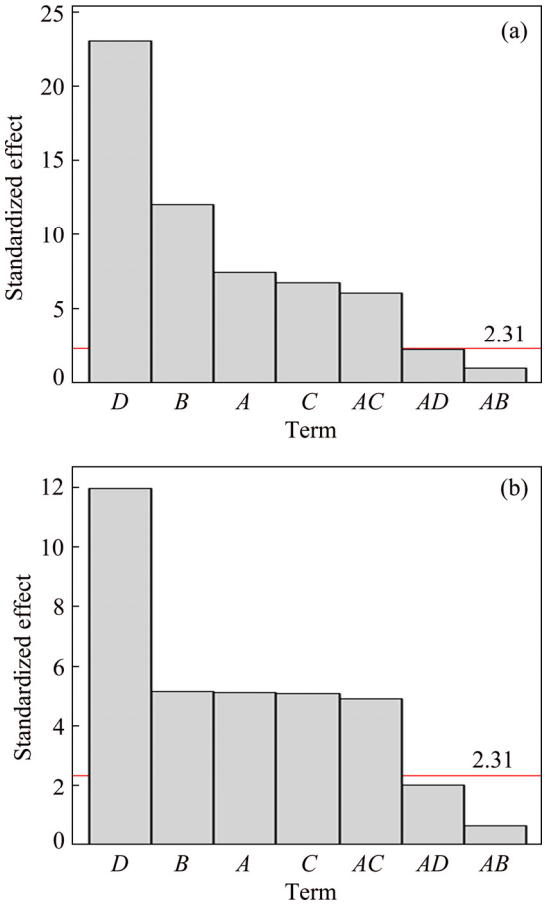

Fig. 5 Pareto chart of elastic modulus (a) and mass loss (b)

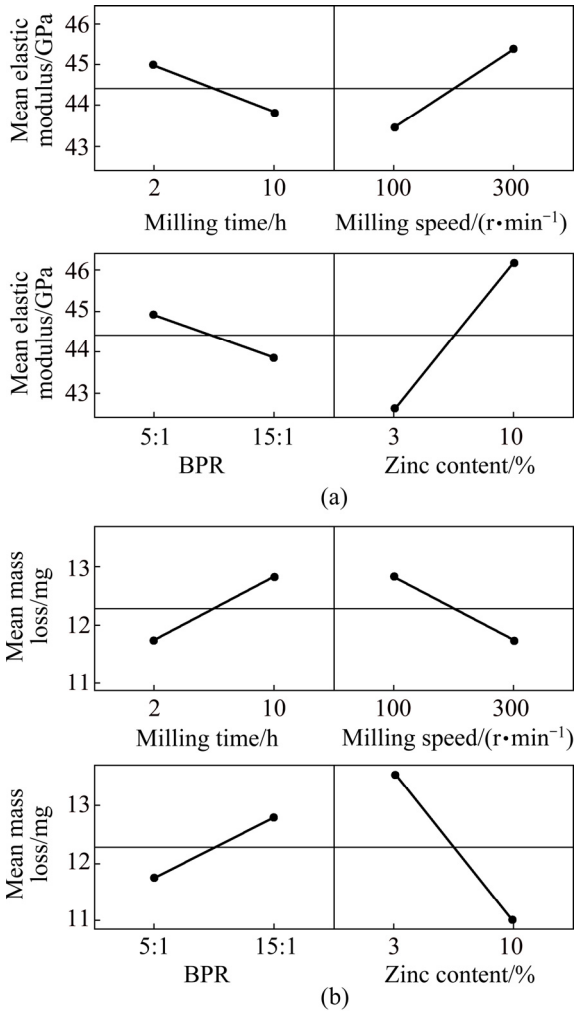

Fig. 6 Main effect plots of elastic modulus (a) and mass loss (b)

other words, higher order interactions such 4-factor interactions were very rare and the contribution to the overall results insignificant residual, which were dispersed randomly.

3.3 Effect of milling time, milling speed, BPR and Zn content on multiple response

The main effect plots of the studied factors were presented in Fig. 6 corresponding to elastic modulus and mass loss, respectively. Due to the fact that hard tissue is mainly affected by compression stress, the elastic modulus of the Mg−Zn alloys was considered. The elastic modulus of human cortical bone is in the range of 30−57 GPa [2]. According to the developed design, the elastic modulus of Mg was slightly increased as Zn was added. Since the modulus of solute Zn atom is higher than pure Mg, thus Zn incorporation mainly increased modulus of Mg. The attained modulus was considerably very close to human bone. In addition, Zn was added in order to reduce the degradation rate of pure Mg [22]. In this study, mass loss was chosen as an indication of corrosion behavior. Lowering of mass loss indicated that the corrosion resistance was improved, accordingly reduced the biodegradation rate during implantation period. On the whole, the degradation rate of pure Mg was capably slowed down by incorporating as low as 3% Zn. As shown in Fig. 6, lowering of milling time and BPR combining with increasing in milling speed and Zn content led to the enhancement of elastic modulus and corrosion resistance of Mg−Zn alloy.

DATTA et al [23] reported that a homogenous alloy mixture of Mg, Zn and Ca was formed up to 1 h of milling without any diffusive or combustion reaction occurring between pure metals which may cause increasing in density. In addition, prolonged milling time up to 8 h resulted in formation of amorphous phase. However, in this present study although the milling time was considerably slightly longer (maximum 10 h), there was no formation of amorphous phase in Mg−Zn alloy, which indicated that no diffusive mixing mechanism was initiated in this binary alloy system within the milling time. Therefore, the results suggested that the milling time used in this work was suitable in order to obtain required elastic modulus and mass loss without formation of any amorphous phase or existence of contaminant.

Main effect plots showed that increasing milling time reduced elastic modulus as shown in Fig. 6(a). As shown in Table 8, the internal strain of 2 h milled alloy was between 0.20% and 0.58%, which then reduced to 0.17% to 0.31% as the mechanical alloying was extended to 10 h. The strain reduction could be explained by the high generation of internal energy during prolong milling which triggered the increasing in temperature during mechanical alloying [24]. In addition, as reported by KIM and BUSH [25], the presence of porosity due to the low densification of alloy effectively reduced the elastic modulus. Lowering of internal strain thus reduced the elastic modulus of the biodegradable alloy.

Table 8 Internal strain of single replication Mg−Zn alloy

Run	Milling time/h	Internal strain/%
1	2	0.20
3	2	0.58
5	2	0.43
7	2	0.36
2	10	0.31
4	10	0.22
6	10	0.17
8	10	0.24

As shown in Fig. 6(b), mass loss of Mg−Zn alloy increased as milling time extended. Increasing in mass loss indicated the lowering of corrosion resistance. This result was probably related to mechanism of work hardening or strain hardening occurred in the powder particles during mechanical alloying of Mg−Zn powder. Hardened Mg−Zn mixture powder provides poor compressibility, which makes it more difficult to be deformed during compaction [26]. This restriction resulted in the formation of pores thus reduced the corrosion resistance of the Mg−Zn alloy especially due to the pitting mechanism.

Based on a study by SHEHATA et al [27], faster milling speed transfers higher kinetic energy into powders and higher kinetic energy leads to the presence of refined microstructure and also decreases the diffusion distance. At higher milling speed, milling process promotes homogenization and alloying occurred. As shown in Fig. 6, increasing in milling speed increased both elastic modulus and corrosion resistance. Table 9 displayed the dislocation density within the grains increased as a function of milling speed. The lowest dislocation density was 1.1503×10^{-6} m^{-2} attained at 100 r/min and the highest dislocation density was 10.2787×10^{-6} m^{-2} achieved at 300 r/min. The increasing in dislocation density resulted in the increasing in elastic modulus. This was due to the increasing in accumulative defect which then mutually blocking the dislocation movement of each other when the external pressure was exerted [28].

Table 9 Dislocation density of single replicate of Mg−Zn alloy

Run	Milling speed/(r·min^{-1})	Dislocation density/10^{-16} m^{-2}
1	100	1.5324
2	100	3.0532
5	100	2.1500
6	100	1.1503
3	300	10.2787
4	300	8.6251
7	300	2.0304
8	300	1.7802

Furthermore, increasing in milling speed up to 300 r/min led to refinement of the particles consequently increased the compressibility of the powder during consolidation. As the compressibility was improved, load bearing area between the particles increased thus reduced the porosity. Reduction of porosity is good for elastic modulus and corrosion resistance improvement [29]. In this study, approximately complete alloying occurred though at milling speed as low as 100 r/min. It can be said that, 100 r/min was sufficient to provide energy in refining the milled grains and initiating the formation of α-Mg solid solution during mechanical alloying and subsequent consolidation. Therefore, the enhancement of elastic modulus and corrosion resistance was attained.

The ratio of the mass of the ball to the powder (BPR) is an important variable in the milling process. In the present work, elastic modulus and corrosion resistance were reduced with the increasing in BPR. This is because of soft and ductile Mg, excessive heat generated during mechanical alloying process with high BPR caused the occurrence of cold welding which then led to the high amount of agglomeration between the particles [23]. Once the severe agglomerated powder formed, the densification of powder and bonding between particles were deteriorated which then resulted in high formation of porosity. High porosity due to the agglomeration of powder consequently caused a reduction in both corrosion resistance and elastic modulus [23,27].

In addition, as shown in Table 10, crystallite enlargement occurred as the BPR was increased up to 15:1. The largest crystallite size of 93.24 nm was seen in sample 6. This sample was mechanically alloyed with 3% Zn for 10 h at 100 r/min using 15:1 of BPR. This suggested that combining high BPR with prolong milling time resulted in high accumulative internal energy during mechanical alloying. High energy generation simultaneously increased the milling temperature thus,

resulted in the enlargement of crystallite size [15]. As the milled powder subsequently consolidated, the crystallite of Mg gradually increased as a function of sintering temperature.

Table 10 Crystallite size of single replicate of Mg−Zn alloy

Run	BPR	Crystallite size/nm
1	3:1	80.78
2	3:1	57.23
3	3:1	28.04
4	3:1	34.05
5	10:1	68.20
6	10:1	93.24
7	10:1	70.18
8	10:1	74.95

The smallest crystallite size of 28.04 nm (sample 3) was achieved when the sample was mechanically alloyed with 10% Zn for 2 h at 300 r/min using 5:1 of BPR. Short duration of mechanical alloying with a low BPR might avoid the generation of excessive heat although the rotational speed was considerably high (300 r/min). Moreover, the refinement of Mg crystallite size of this sample was supported by the addition of high Zn content. In fact, the crystallite refinement caused the increasing in crystallite number per volume, therefore the concentration of grain boundary was proportionally increased. Increasing in grain boundary concentration reduced the grain boundary width, thus led to the increasing in elastic modulus [29].

Figure 6 displays that increasing the amount of Zn increased both elastic modulus and corrosion resistance of Mg alloy. Zn was added into pure Mg in order to improve its mechanical properties by forming Mg−Zn alloy. Higher Zn content means that there are more solute Zn atoms that could restrict dislocation motion in the Mg lattice structure leading to an improvement in modulus [30]. Addition of Zn remarkably refines crystallite size of Mg by hindering the grain boundary expansion which contributed to the increase in mechanical strength [16,31] obeying the Hall−Petch formula. From XRD analysis, Zn element mainly resolved in primary Mg forming α-Mg when Zn content was 3% which can improve the strength of the alloy by solid solution strengthening. When Zn content was increased to 10%, a mixture of α-Mg solid solution and γ-MgZn phase precipitated in the matrix which enhanced the elastic modulus and strength by a dispersion strengthening [32,33]. In most cases, the presence of secondary phase needs to be avoided due to its hard and brittle properties, which inhibits the dislocation recovery and increases dislocation density thus contributes to the reduction of the elongation.

Table 11 showed the effect of Zn content on the relative density of the alloys, it was discovered that the existence of γ-MgZn phase deteriorated the theoretical density of the alloys, which was not beneficial for mechanical properties. Maximum relative density of Mg−10%Zn (87.45%) was lower than the minimum relative density of Mg−3%Zn (94.76%). The low relative density suggested that the high porosity in the 10% Zn alloy was due to the association of γ-MgZn phase in the Mg metallic which was supported by XRD analysis. The compressibility of soft Mg matrix during consolidation was inhibited by secondary metallic phase MgZn which explained the low relative density with high content of Zn.

Table 11 Relative density of single replicate of Mg−Zn alloy

Run	w(Zn)/%	Relative density/%
1	3	94.76
4	3	97.40
6	3	95.03
7	3	95.19
2	10	82.76
3	10	87.45
5	10	84.10
8	10	81.65

However, the result exhibited considerably different effects of Zn content on the studied responses with the presence of γ-MgZn phase. The influence of alloying element from different groups provides different effects on elastic modulus according to valence shell electrons. The addition s-block element into Mg results in a lower elastic modulus than the addition of p- and d-block elements [34]. Thus, addition of Zn effectively resulted in alteration of elastic modulus as Zn is d-block element. As shown in Table 12, increasing Zn content led to a reduction of the lattice constant corresponding to both a and c. The change of lattice parameter of Mg is due to the addition of alloying element in comparison with the

Table 12 Lattice parameters of single replicate of Mg−Zn alloy

Run	w(Zn)/%	a/Å	c/Å	a/c
1	3	3.2028	5.2096	1.626
4	3	3.1917	5.1813	1.623
6	3	3.2068	5.2143	1.626
7	3	3.2007	5.1974	1.624
2	10	3.1597	5.1124	1.618
3	10	3.1539	5.0966	1.616
5	10	3.1648	5.1253	1.619
8	10	3.1702	5.1397	1.621

atomic radius of solute atom from the hcp structure. The atomic radii of Mg and Zn are 157 pm and 134 pm respectively, where the radius difference was only 14.10%, thus substitutional solid solution strengthening was anticipated to occur, where this condition obeyed the Hume−Rothery rule. As the Zn atom was smaller than Mg atom, the substitution of solute Zn on Mg solvent resulted in reducing the Mg lattice.

As depicted in Table 12, the maximum reductions of a and c lattice constants for 3% Zn addition were 3.1917 Å and 5.1813 Å, whereas as the Zn content was incorporated up to 10%, the a and c lattice constants continually reduced to 3.1539 Å and 5.0966 Å respectively. No significant change of c/a ratio was observed in the case of 3% Zn; however, with 10% Zn addition, c/a ratio slightly reduced as the lattice parameter reduced. The decrease in lattice constant results in an increase in the elastic modulus. This condition is owing to the shortening of the nearest-neighbour distance between Mg and the alloying element [35].

In addition, the reduction of lattice parameter indicated more solute atom dissolved in the solvent lattice. The more Zn dissolved in Mg lattice, the more effect on its bulk properties might achieved. Regardless of γ-MgZn phase, the addition of 10% Zn was considerably useful for enhancing elastic modulus and corrosion resistance. In the case of corrosion behaviour, high Zn content prompted the formation of protective layer particularly during the usage in corrosive or aggressive surroundings.

In the considered range parameter, principal factor of Zn content was the most significant variable in achieving maximum elastic modulus and attaining mostly enhanced corrosion resistance corresponding to minimum mass loss. According to the ascending effect of this parameter, increasing in Zn amount enhanced Mg−Zn alloy elastic modulus since Zn element has higher elastic modulus compared with Mg. Moreover, the smaller substituted Zn atom in the Mg crystal structure resulted in contraction of the lattice thus, increasing the intrinsic modulus of the Mg−Zn alloy. Increasing in Zn content resulted in lowering mass loss during immersion in 3.5% NaCl solution. Reduction of mass loss of the Mg−Zn alloy showed the beneficial effect of Zn element on the formation of a protective film on the surface of alloys. Addition of 10% Zn in the Mg matrix exhibited the higher corrosion resistance than 3% Zn addition. However, most of previous works reported that further increase in Zn content higher than 12% might deteriorate the corrosion rate which was driven by galvanic couple effect [36,37].

On the other hand, as shown in Fig. 7, the peaks of γ-MgZn phase started to form during mechanical alloying when 10% Zn was incorporated, consequently affected the compressibility of alloy powder. The intensity of peaks of the sintered alloy increased which consequently influenced its final properties. In most cases, secondary phase that existed in the metallic matrix provided strengthening effect due to its inherent hard and brittle properties of intermetallic compound [30]. However, as reported by ZHANG et al [33], formation of secondary phase in the Mg matrix commonly deteriorated machinability of Mg alloys due to reduction of its elongation. In this study, compressibility of alloy powders was reduced with the presence of γ-MgZn compound which resulted in lowering the densification of the alloy compacts. Thus, the addition of Zn in the present work must be strictly controlled in order to improve the required properties without sacrificing its ductility too much.

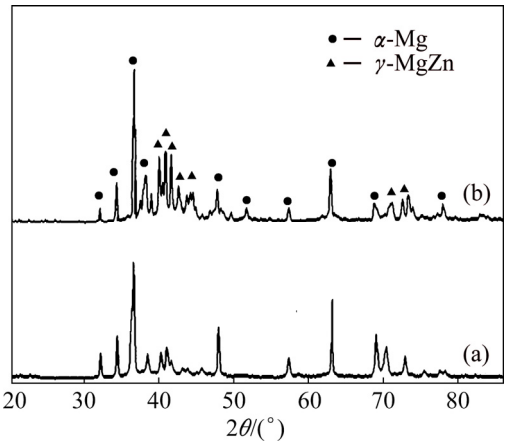

Fig. 7 XRD patterns of as-milled alloy powders of Mg−3%Zn (a) and Mg−10%Zn (b)

4 Conclusions

A reliable statistical model based on fractional factorial experiment design has been developed which can be applied for the optimization of binary Mg−Zn alloy synthesized by mechanical alloying. In the present work, elastic modulus of biodegradable Mg−Zn alloy was obtained between 40.18−47.88 GPa which resembled to natural bone (i.e., 30−57 GPa). Corrosion mass loss of pure Mg (33.74 mg) was reduced with addition of 3%−10% Zn which was between 9.32 and 15.38 mg. Experimental design using 2^{4-1} fractional factorial design enabled to establish the polynomial functions that described the effects of processing condition on the elastic modulus and mass loss of Mg−Zn alloy prepared by mechanical alloying and subsequent consolidation. The statistical analysis demonstrated main factor of milling time, milling speed, ball to powder mass ratio and Zn content and only the interaction of milling time and ball to powder mass ratio

(AB) was significant for both responses density and hardness as the *P*-value is less than 0.05. The higher order interactions such 4-factor interactions were very rare and considerably negligible. In short, mechanical properties (represented by elastic modulus) and corrosion resistance (represented by weight loss) of biodegradable Mg−Zn alloy can be statistically predicted according to the developed models.

Acknowledgement

This work was supported by the Universiti Sains Malaysia RU-PRGS (No. 8046026) and Universiti Sains Malaysia FRGS by Ministry of High Education, Malaysia (No. 6071304).

References

[1] WITTE F, KAESE V, HAFERKAMP H, SWITZER E, LINDENBERG A M, WIRTH C J, WINDHAGEN H. In vivo corrosion of four magnesium alloys and the associated bone response [J]. Biomaterials, 2005, 26: 3557−3563.

[2] ZENG Rong-chang, DIETZEL W G, WITTE F, HORT N, BLAWERT C. Progress and challenge for magnesium alloys as biomaterials [J]. Advanced Engineering Materials, 2008, 10: B3−B14.

[3] LI Wen, GUAN Shao-kang, CHEN Juan, HU Jun-hua, CHEN Shuai, WANG Li-guo, ZHU Shi-jie. Preparation and in vitro degradation of the composite coating with high adhesion strength on biodegradable Mg−Zn−Ca alloy [J]. Materials Characterization, 2011, 62: 1158−1165.

[4] HOU L, LI Z, ZHAO H, PAN Y, PAVLINICH S, LIU X, LI X, ZHENG Y, LI L, Microstructure, mechanical properties, corrosion behavior and biocompatibility of as-extruded biodegradable Mg−3Sn−1Zn−0.5Mn alloy [J]. Journal of Materials Science and Technology, 2016, 32: 874−882.

[5] BAKHSHESHI-RAD H R, IDRIS M H, ABDUL-KADIR M R, OURDJINI A, MEDRAJ M, DAROONPARVAR M, HAMZAH E. Mechanical and bio-corrosion properties of quaternary Mg−Ca−Mn−Zn alloys compared with binary Mg−Ca alloys [J]. Materials and Design, 2014, 53: 283−292.

[6] LI Tao, ZHANG Hai-long, HE Yong, WEN Ning, WANG Xi-tao. Microstructure, mechanical properties and in vitro degradation behavior of a novel biodegradable Mg−1.5Zn−0.6Zr−0.2Sc alloy [J]. Journal of Materials Science and Technology, 2015, 31: 744−750.

[7] PLUM L M, RINK L, HAASE H. The essential toxin: Impact of zinc on human health [J]. International Journal of Environmental Research and Public Health, 2010, 7: 1342−1365.

[8] GU Xue-nan, ZHENG Yu-feng, CHENG Yan, ZHONG Sheng-ping, XI Ting-fei. In vitro corrosion and biocompatibility of binary magnesium alloys [J]. Biomaterials, 2009, 30: 484−498.

[9] XU Zhi-gang, HODGSON M A, CAO Peng. Effects of mechanical milling and sintering temperature on the densification, microstructure and tensile properties of the Fe−Mn−Si powder compacts [J]. Journal of Materials Science and Technology, 2016, 32: 1161−1170.

[10] RAMKUMAR K R, ILANGOVAN S, SIVASANKARAN S, ALABOODI A S. Experimental investigation on synthesis and structural characterization of Cu−Zn−*x*wt%Al_2O_3 (*x*=0, 3, 6, 9 & 12%) nanocomposites powders through mechanical alloying [J]. Journal of Alloys and Compounds, 2016, 688: 518−526.

[11] MONTGOMERY D C. Design and analysis of experiments [M]. 8th ed. New York: John Wiley and Sons, 2013.

[12] SALLEH E M, HUSSAIN Z, RAMAKRISHNAN S, GEPREEL M A H. A statistical prediction of density and hardness of biodegradable mechanically alloyed Mg−Zn alloy using fractional factorial design [J]. Journal of Alloys and Compounds, 2015, 644: 476−484.

[13] SATHEESHKUMAR V, LAKSHMINARAYANAN P R. Developing mathematical models on tensile strength and acoustic emission count of ZE41a cast magnesium alloy [J]. Journal of Alloys and Compounds, 2012, 537: 35−42.

[14] KARIMZADEH F, ENAYATI M H, TAVOOSI M. Synthesis and characterization of Zn/Al_2O_3 nanocomposite by mechanical alloying [J]. Materials Science and Engineering A, 2008, 486: 45−48.

[15] NEVES F, BRAZ FERNANDES F M, MARTINS I, CORREIA J B. Parametric optimization of Ti−Ni powder mixtures produced by mechanical alloying [J]. Journal of Alloys and Compounds, 2011, 509: 271−274.

[16] ESKANDARANY M S E. Mechanical alloying for fabrication of advanced engineering materials [M]. New York: William Andrew Publishing, 2001.

[17] ZUHAILAWATI H, MAHANI Y. Effects of milling time on hardness and electrical conductivity of in situ Cu−NbC composite produced by mechanical alloying [J]. Journal of Alloys and Compounds, 2009, 476:142−146.

[18] RAJABI M, SEDIGHI R M, RABIEE S M. Thermal stability of nanocrystalline Mg-based alloys prepared via mechanical alloying [J].Transactions of Nonferrous Metals Society of China, 2016, 26: 398−405.

[19] GUPTA M, SHARON N M L. Magnesium, magnesium alloys, and magnesium composites [M]. New Jersey: John Wiley and Sons, 2011.

[20] MADAVALI Babu, LEE Jin-He, LEE Jin-Kyu, CHO Kuk-Young, SURYANARAYANA C, HONG Soon-Jik, Effects of atmosphere and milling time on the coarsening of copper powders during mechanical milling [J]. Powder Technology, 2014, 256: 251−256.

[21] NAG S, BANERJEE R, FRASER H L. A novel combinatorial approach for understanding microstructural evolution and its relationship to mechanical properties in metallic biomaterials [J]. Acta Biomaterialia, 2007, 3: 369−376.

[22] MUTHUKUMAR M, MOHAN R D, Optimization of mechanical properties of polymer concrete and mix design recommendation based on design of experiments [J]. Journal of Applied Polymer Science, 2004, 94: 1107−1116.

[23] DATTA M K, CHOU D T, HONG D, SAHA P, CHUNG S J, LEE B, SIRINTERLIKCI A, RAMANATHAN M, ROY A, KUMTA P N. Structure and thermal stability of biodegradable Mg−Zn−Ca based amorphous alloys synthesized by mechanical alloying [J]. Materials Science and Engineering B, 2011, 176: 1637−1643.

[24] YUAN Yan-bo, WANG Zhi-wei, ZHENG Rui-xiao, HAO Xiao-ning, AMEYAMA K, MA Chao-li. Effect of mechanical alloying and sintering process on microstructure and mechanical properties of Al−Ni−Y−Co−La alloy [J]. Transactions of Nonferrous Metals Society of China, 2014, 24: 2251−2257.

[25] KIM H S, BUSH M B. The effects of grain size and porosity on the elasticmodulus of nanocrystalline materials [J]. Nanostructured Materials, 1999, 11: 361−367.

[26] SURYANARAYANA C. Mechanical alloying and milling [J]. Progress in Materials Science, 2001, 46: 1−184.

[27] SHEHATA F, FATHY A, ABDELHAMEED M, MOUSTAFA S F. Preparation and properties of Al_2O_3 nanaoparticle reinforced copper matrix composites by in situ processing [J]. Materials and Design, 2009, 30: 2756−2762.

[28] DESCHAMPS A, FRIBOURG G, BRECHET Y, CHEMIN J L, HUTCHINSON C R. In situ evaluation of dynamic precipitation during plastic straining of an Al−Zn−Mg−Cu alloy [J]. Acta Materialia, 2012, 60: 1905−1916.

[29] MASROOR M, SHEIBANI S, ATAIE A. Effect of milling energy on preparation of Cu−Cr/CNT hybrid nano-composite by mechanical alloying [J]. Transactions of Nonferrous Metals Society of China, 2016, 26: 1359−1366.

[30] ZUHAILAWATI H, SALIHIN H M, MAHANI Y. Microstructure and properties of copper composite containing in situ NbC reinforcement: Effects of milling speed [J]. Journal of Alloys and Compounds, 2010, 489: 369−374.

[31] TANE M, KIMIZUKA H, HAGIHARA K, SUZUKI S, MAYAMA T, SEKINO T, NAGAI Y. Effects of stacking sequence and short-range ordering of solute atoms on elastic properties of Mg−Zn−Y alloys with long-period stacking ordered structures [J]. Acta Materialia, 2015, 96: 170−188.

[32] TAN Li-li, YU Xiao-ming, WAN Peng, YANG Ke. Biodegradable materials for bone repairs: A review [J]. Journal of Materials Science and Technology, 2013, 29: 503−513.

[33] ZHANG Shao-xiang, ZHANG Xiao-nong, ZHAO Chang-li, LI Jia-nan, SONG Yang, XIE Chao-ying, TAO Hai-rong, ZHANG Yan, HE Yao-hua, JIANG Yao, BIAN Yu-jun. Research on an Mg−Zn alloy as a degradable biomaterial [J]. Acta Biomaterilia, 2010, 6: 626−640.

[34] TODA-CARABALLO I, GALINDO-NAVA E I, RIVERA-DIAZ-DEL-CASTILLO P E J, TODA-CARABALLO ISAAC, GALINDO-NAVA ENRIQUE I, RIVERA-DIAZ-DEL-CASTILLO PEDRO E J. Understanding the factors influencing yield strength on Mg alloys [J]. Acta Materialia, 2014, 75: 287−296.

[35] GANESHAN S, SHANG S L, WANG Y, LIU Z K. Effect of alloying elements on the elastic properties of Mg from first-principles calculations [J]. Acta Materilia, 2009, 57: 3876−3884.

[36] ZHOU Bi-cheng, SHANG Shun-li, WANG Yi, LIU Zi-kui. Diffusion coefficients of alloying elements in dilute Mg alloys: A comprehensive first-principles study [J]. Acta Materialia, 2016, 103: 573−586.

[37] NARAYANASAMY P, SELVAKUMAR N. Tensile, compressive and wear behaviour of self-lubricating sintered magnesium based composites [J]. Transactions of Nonferrous Metals Society of China, 2017, 27: 312−323.

机械合金化制备可降解 Mg−Zn 合金：用分式析因设计对其弹性模量和质量损失进行统计预测

Emee Marina SALLEH[1,2], Hussain ZUHAILAWATI[1], Sivakumar RAMAKRISHNAN[1]

1. Biomaterials Niche Area, School of Materials and Mineral Resources Engineering, Engineering Campus, Universiti Sains Malaysia, 14300 Nibong Tebal, Penang, Malaysia;
2. School of Applied Physics, Faculty of Science and Technology, Universiti Kebangsaan Malaysia, 43600 UKM Bangi, Selangor, Malaysia

摘　要：用机械合金化方法制备可降解 Mg−Zn 合金，并用分式析因设计法建立统计学模型来预测块体合金的弹性模量和腐蚀质量损失。研究机械合金化参数(球磨时间、球磨速度、球料比和 Zn 含量)及其交互作用对合金性能的影响，共涉及 4 因素 2 次重复，因此进行了 16 次 2 水平分式析因设计。方差分析(ANOVA)、 回归分析和 R^2 测试结果表明此模型预测精度高。统计模型预测的可降解 Mg−Zn 合金的弹性模量为 40.18~47.88 GPa，类似于自然骨 (30−57 GPa)。添加质量分数为 3%~10% Zn(9.32~15.38 mg)后，可以改善合金的耐腐蚀性能，腐蚀后纯 Mg 质量损失约 33.74 mg。最显著的自变量是 Zn 含量，且只有球磨时间和球料比的交互作用具有显著性，P 值小于 0.05。建立的模型可以从统计学上有效预测可降解 Mg−Zn 合金的力学性能(通过弹性模量反映)和耐腐蚀性能(通过重量损失反映)。

关键词：可降解 Mg−Zn 合金；机械合金化；分式析因设计；弹性模量；质量损失

(Edited by Xiang-qun LI)